RSC Advances

PAPER

View Article Online
View Journal | View Issue

Cite this: *RSC Adv.*, 2023, **13**, 6171

Morphological, cytotoxicity, and coagulation assessments of perlite as a new hemostatic biomaterial

Esmaeil Biazar, *[a] Saeid Heidari Keshel,*[bc] Vahid Niazi,[de] Nader Vazifeh Shiran,[f] Roxana Saljooghi,[a] Mina Jarrahi[a] and Ahmad Mehdipour Arbastan[g]

Received 7th December 2022
Accepted 13th February 2023

DOI: 10.1039/d2ra07795g

rsc.li/rsc-advances

Hemorrhage control is vital for clinical outcomes after surgical treatment and pre-hospital trauma injuries. Numerous biomaterials have been investigated to control surgical and traumatic bleeding. In this study, for the first time, perlite was introduced as an aluminosilicate biomaterial and compared with other ceramics such as kaolin and bentonite in terms of morphology, cytotoxicity, mutagenicity, and hemostatic evaluations. Cellular studies showed that perlite has excellent viability, good cell adhesion, and high anti-mutagenicity. Coagulation results demonstrated that the shortest clotting time (140 seconds with a concentration of 50 mg mL^{-1}) was obtained for perlite samples compared to other samples. Therefore, perlite seems most efficient as a biocompatible ceramic for hemorrhage control and other biomaterial designs.

1. Introduction

Biomaterials have been applied in civilian and military settings with less investigation for the latter.[1] One typical example is the biomaterials used for hemorrhage control in surgeries in hospital settings and for combat casualty care on a battlefield.[2] Tremendous advances in this area have been made to improve health care and life-saving in civilian communities and military operations.[3,4] Uncontrolled bleeding from trauma is the second leading cause of death in the civilian community after central nervous system injuries[5] and the primary reason for dying on the battlefield, followed by brain injuries.[6] Many biomaterials in different forms have been studied to control various types of bleeding. These materials are classified according to their forms and types such as hemostatic dressings,[7–10] solid particles or powders,[11–15] fibers,[16] hydrogels,[17–19] liquid tissue sealants,[20–22] and dispersions,[23] made from natural or synthetic polymers, ceramics and their combinations, and bioadhesives.[23–25] One of the ceramics proposed as a hemostatic agent is aluminosilicate combination. Aluminosilicates absorb water from wounds and their surrounding due to their chemical and structural properties, and thus, increase the concentration of coagulation factors and accelerate this procedure. So overall, these materials are influenced by two mechanisms: the activation of platelets and their effects on the coagulation cascade.[26,27]

Zeolites are another group of aluminosilicates. About 40 natural zeolites have been known and 150 types of zeolites have been synthesized.[28] A zeolite-based product with the brand name QuikClot™ (QC) was proposed as a hemostatic agent by Z-Medica Inc., Newington, CT, USA. This microporous crystalline aluminosilicate product has been able to control bleeding in various animal bleeding models and even clinically, it has shown good hemostatic properties.[29–31] At that time the use of known hemostatic agents such as QuikClot was associated with tissue damage caused by the exothermic reaction.[29,32–34]

Wound Stat (WoundStat™; WS) is another minerals-based product (Trauma Cure Inc., Bethesda, MD), as a hemostatic agent consisting of a granular combination of a smectite mineral and a superabsorbent polyacrylate.[35–37] The results of swine models of femoral arteriotomy showed that this product is an effective local hemostatic agent.[37,38] Other ceramics such as hydroxyapatite has been used to control bleeding in osteoporotic sternums.[26,27] However, their suitability for severe bleeding has not been demonstrated. Another hemostatic powder (Hemospray; Cook Medical, Winston-Salem, NC, USA), which was granted clearance for clinical use by the U.S. Food and Drug Administration for endoscopic therapy of nonvariceal

[a]*Biomaterials and Tissue Engineering Group, Department of Biomedical Engineering, Islamic Azad University, Tonekabon Branch, Tonekabon, Iran. E-mail: e.biazar@toniau.ac.ir; kia_esm@yahoo.com; Fax: +981154271105; Tel: +981154271105*

[b]*Department of Tissue Engineering and Applied Cell Sciences, School of Advanced Technologies in Medicine, Shahid Beheshti University of Medical Sciences, Tehran, Iran. E-mail: saeed.heidari@sbmu.ac.ir; Fax: +989125870517; Tel: +989125870517*

[c]*Medical Nanotechnology and Tissue Engineering Research Center, Shahid Beheshti University of Medical Sciences, Tehran, Iran*

[d]*Stem Cell Research Center, Golestan University of Medical Science, Gorgan, Iran*

[e]*Department of Molecular Medicine, Faculty of Advanced Medical Technologies, Golestan University of Medical Science, Gorgan, Iran*

[f]*Department of Hematology and Blood Banking, Faculty of Medical Sciences, Tarbiat Modares University, Tehran, Iran*

[g]*School of Medicine, Faculty of Medical Sciences, Islamic Azad University, Tonekabon Branch, Tonekabon, Iran*

GI hemorrhage, consisted of an inert, nontoxic powder called bentonite from aluminosilicate family.[39] Mortazavi *et al.* showed that a specific mixture of bentonite–zeolite minerals has a significant effect in shortening the bleeding time and can also significantly reduce the blood clotting time.[40] Kaolin is prepared as a bioceramic from the family of layered aluminosilicates $[Al_4(Si_4O_{10})(OH)_8]$ from the weathering of the feldspar mineral group.[25] Kaolin, an aluminum phyllosilicate clay mineral, is a potent cation-based activator of the intrinsic pathway of coagulation. The nongranular nature of the product also allows for removal of the product without leaving residue or granules that could potentially promote thrombosis.[6,37,39] By enhancing the intrinsic clotting cascade, kaolin-impregnated gauze promotes the development of hemostatic clots that form following a brief period of postapplication hemorrhage. A potential shortcoming is that kaolin relies on the presence of active clotting factors to regulate the speed of clot formation. For this reason, its efficacy may be significantly reduced in the setting of functional or dilutional coagulopathy.[36] Kheirabadi *et al.* examined the safety of two effective hemostatic agents WS and Combat Gauze (CG) in a surgical model. The results showed local tissue damage and embolization to distal organs as the result of treatment with the agents. Although no significant difference was observed between CG and conventional gauze, WS caused severe endothelial injury and significant intermural damage, which made the vessels refractory to primary surgical repair. The WS residues were also embolized in the venous circulation and trapped in the lung with associated thrombosis. If used in a wound, it may be necessary to replace the injured vessels with interposition grafts to avoid thrombotic complications.[41,42] Bowman *et al.* investigated the cellular toxicity of WS and other minerals such as bentonite, kaolin, and QuikClot ACS+ (QC+). The results showed that aluminum silicates are relatively innocuous to epithelial cells, all produced some toxicity toward endothelial cells and macrophages. WS and bentonite were significantly more toxic than kaolin and zeolite present in QC+, respectively, at equivalent doses.[43]

Perlite as an aluminosilicate combination is a glassy volcanic rock, customarily light gray, with a rhyolitic composition and 2–5% of combined water. Perlite commercially includes any volcanic glass that expands when heated quickly, forming a lightweight, frothy material. According to the fact that most perlites have a high silica content, usually greater than 70%, and are adsorptive. They are chemically inert in many environments and hence are excellent filter aids and fillers in various ceramics processing.[44] Perlite has been studied intensively due to its structural properties, chemical compositions, and surface chemical properties. In this study, we first time introduced perlite as a biomaterial for blood coagulation and investigated some of its properties by different analyses such as toxicity, mutagenesis, and hemostatic analyses compared to commercial samples.

2. Materials and methods

2.1. Preparation of microparticle powders

Perlite, kaolin, and bentonite samples were prepared from Iran mines [Iran, Maragheh]. For the preparation of powders, 2 g of the pure materials were introduced into a grinding mill with the tungsten carbide balls in a powder/ball ratio of 1 : 15 (w/w). Then, they were mechanically activated for different periods of time. All powders were treated as follows: the suspension containing 10 g per liter of powder was mechanically stirred for 24 hours, and then the full suspensions were filtered through filter paper. The suspension was dried for 24 hours at 100 °C to obtain a dry powder for the experiments (Fig. 1).

2.2. Morphological studies

The elemental composition of the natural powders was determined by X-ray Fluorescence (XRF, PERFORM, X, Thermo Fisher, USA). The morphology of the powders was examined by scanning electron microscope (Cambridge Stereo-scan, S-360, Wetzlar, Germany). The powders were gold-sputtered (Ion Sputter, JFC-1100, JOEL, Japan) to provide surface conduction before scanning. The powders were dried under nitrogen gas to measure the specific surface area of the samples by BET analysis (BEL Inc. Japan).

2.3. Cytotoxicity test

The fibroblast cells suspension (L929, mouse tail) was prepared according to the ISO10993 standard. The suspension was transferred to a flask (25 mL) containing 5 mL Dulbecco's Modified Eagle's Medium (DMEM; L-glutamine, penicillin, streptavidin) and 10% fetal bovine serum (FBS). The suspension was then placed in an incubator (5% CO_2, 37 °C). The fibroblast cells were proliferated in the flask and were washed using FBS/

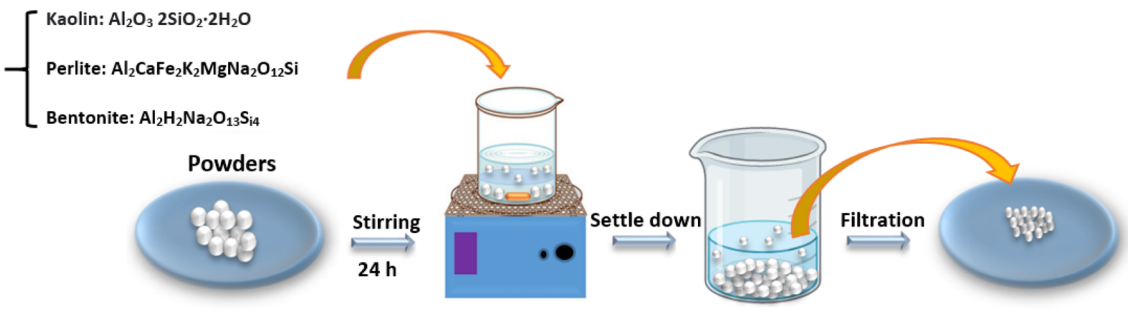

Fig. 1 Schematic image of the process of preparing microparticles.

ethylene diamine tetraacetic acid (EDTA). Then the trypsin enzyme/EDTA was added to the flask (4 °C), and the flask was incubated for 2 minutes. The culture media (FBS/DMEM) was added to the flask, and the cells were gently pipetted. The cell suspension was transferred to a falcon tube (15 mL) and centrifuged (1410 rpm) for 5 minutes. The solution was removed, and the precipitation was transferred to a new flask (75 mL) for re-culturing. Cells from the Petri dish (control: TCPS) and the main sample were placed individually in one of the Petri dish wells using a sterilized pincer. 100 000 cells per well were seeded into a 24-well culture plate removed by pipette and poured onto the control and the main samples. Then all samples were placed in a Memmert incubator at 37 °C for 48 hours and studied using a ceti microscope (Wolf Laboratories, UK). Cell proliferation was determined by 3-(4,5-dimethylthiazol-2-yl)-2,5-diphenyltetrazolium bromide (MTT) assay for viable cell numbers. The MTT compound is converted to colored formazan by living cells that is soluble in tissue culture medium. The quantity of formazan product is directly proportional to the number of viable cells in the culture. The assays were performed by adding 1 mL of MTT solution (Sigma, St. Louis, MO) and 9 mL fresh medium to each well after aspirating the spent medium and incubating at 37 °C for 4 hours with protection from light. Colorimetric measurement of formazan dye was performed at a wavelength of 606 nm using a ray to microplate reader. For microscopic study, the cultured scaffolds with cells were washed with PBS and then fixed with glutaraldehyde (2.5%) at 4 °C for 2 hours. The samples were dehydrated by alcohols. To dehydrate the samples, an ascending gradient of ethanol in dilutions of 30–50–60–80% was used in each step for 5 minutes and then 100% ethanol for 30 seconds. The samples were exposed to tetraoxide osmium vapors at 4 °C for 2 hours and then coated with gold and investigated by a scanning electron microscope (TScan, VEGA, Czech).

Table 1 XRF results of studied samples

%	Perlite	Kaolin	Bentonite
SiO_2	74.21	61.51	71.61
Al_2O_3	13.81	24.53	22.01
Fe_2O_3	0.89	0.55	1.81
Na_2O	2.91	0.81	1.00

2.4. Ames test

The powders (25 mg mL^{-1}) were subsequently evaluated in terms of anti-mutagenicity and anti-cancer properties by the standard reverse mutation assay (Ames test).[44,45] *Salmonella typhimurium* TA100 was used for the study. Fresh bacterial culture was used for the test, and incubation time for the culture in nutrient broth was not more than 16 hours. Appropriate bacterial concentration was estimated by cells at mL. According to Ames, fruit juice was added to test tube containing 0.5 mL of the overnight fresh bacterial culture, 0.5 mL of histidine and biotin solution (0.5 mM histidine/0.5 N biotin), 10 mL top agar (50 g per L agar + 50 g per L NaCl), sodium azide as a carcinogen (1.5 μg per mL sodium azide) and then content of this tube distributed on the surface of minimum medium of glucose agar (% 40 glucose), after 3 seconds shaking incubation was performed at 37 °C for 48 hours. Each treatment has been repeated three times. After 48 hours, reversed colonies were counted in control and test plates, and after angular conversion, results were compared with variance analysis. In terms of carcinogenic effects, most of the materials were inactive in their original form and had to become metabolically active to display mutagenesis properties. So it was necessary to add a microsomal sterile fruit juice from mammalian tissue such as a rat. After 10 hours. Starvation, livers of rats separated. Starvation stimulates and enhances liver enzyme secretion. Livers were homogenized in potassium chloride 0.15 M and centrifuged at 9000 rpm and 4 °C for 10 minutes. The supernatant (S9 mixture) was removed and mixed with necessary cofactors NADP and G-6p (glucose-6 phosphate) and then added to the top agar to evaluate anti-cancer properties. Also, after counting colonies in anti-cancer and anti-mutagenesis tests, prevention percentage or antioxidant activity[44,45] has been calculated as follows (eqn (1)):

$$\text{Prevention percent} = \left(1 - \frac{T}{M}\right) \times 100 \quad (1)$$

T shows reversed colonies in each Petri dish under carcinogen and samples, and M represents reversed colonies in Petri dishes related to a positive control (mutagen).

2.5. Hemostatic analyze

Thrombogenic effects of the studied materials were compared with the CT test. For this purpose, 200 mg of each powder was

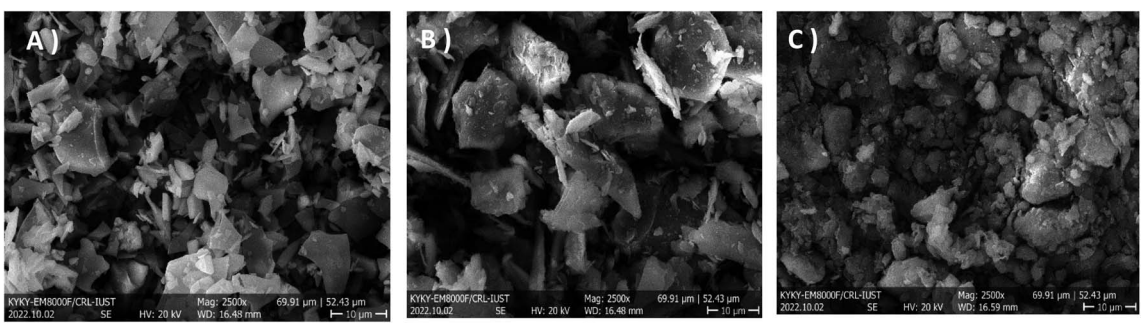

Fig. 2 Microscopic images from powders: (A) Perlite, (B) Kaolin, and (C) Bentonite (mag.: 2500×).

added to 1000 μL of normal saline, then 30, 60, 120, 250, 500, and 1000 microliters of the above mixture were transferred to each tube (respectively containing 12, 25, 50, 100 and 200 mg) so that the volume of all tubes was reached to 1000 μL with normal saline. Only 1000 μL of normal saline was added to the control tube. The tubes were incubated for 12 hours at 37 °C until 80% of the normal saline evaporated, and the stimulating powders remained wet at the bottom of the tube to be ready for the test. Polystyrene plastic tubes (gamma tubes) were used in all conditions to eliminate the effect of glass in coagulation activation. About 12 mL of blood samples were taken from healthy people (average: 28 years) (blood entering the syringe equals the start of time measurement) and were added to each tube and incubated at 37 °C. After 3 minutes from the start of the chronometer, the triplicate tubes were removed from the bain-marie every 30 seconds. The appearance of clots on their walls was visually checked, and the average coagulation time (CT) was recorded. The experiment referred to different values of powders. The values for all samples were evaluated as the mean ± standard deviation (SD). Statistically significant differences, $p < 0.05$ in a time group and $p < 0.01$ between groups were investigated using Student's *t*-test and two-way analysis of variance (ANOVA) with Tukey's *post hoc* multiple comparison test for all groups.

The samples were measured for a variety of biochemical components (albumin, alkaline phosphatase, amylase, total bilirubin, calcium, chloride, cholesterol, creatine kinase, creatinine, gamma-glutamyltransferase [GGT], glucose, ASAT, alanine aminotransferase [ALAT], hydroxybutyrate dehydrogenase [HBDH], LDH, lipase, *p*-amylase, phosphate, potassium, sodium, total protein, triglyceride, urea, and uric acid and other elements) using Roche/Hitachi 917 System (Roche Diagnostics, Mannheim, Germany).

2.6. Statistical analyze

The values for all samples were evaluated as the mean ± standard deviation (SD). Statistically significant differences; $p < 0.05$

Table 2 Specific surface area characteristics of clays calculated from nitrogen sorption isotherms

Sample	BET surface area ($m^2\ g^{-1}$)	Pore volume ($cm^3\ g^{-1}$)	Pore diameter (nm)
Perlite	26.22 ± 0.31	2.07 ± 0.05	15 ± 0.68
Kaolin	17.11 ± 1.01	0.06 ± 0.01	3.4 ± 0.11
Bentonite	14.46 ± 1.03	0.04 ± 0.01	3.6 ± 0.21

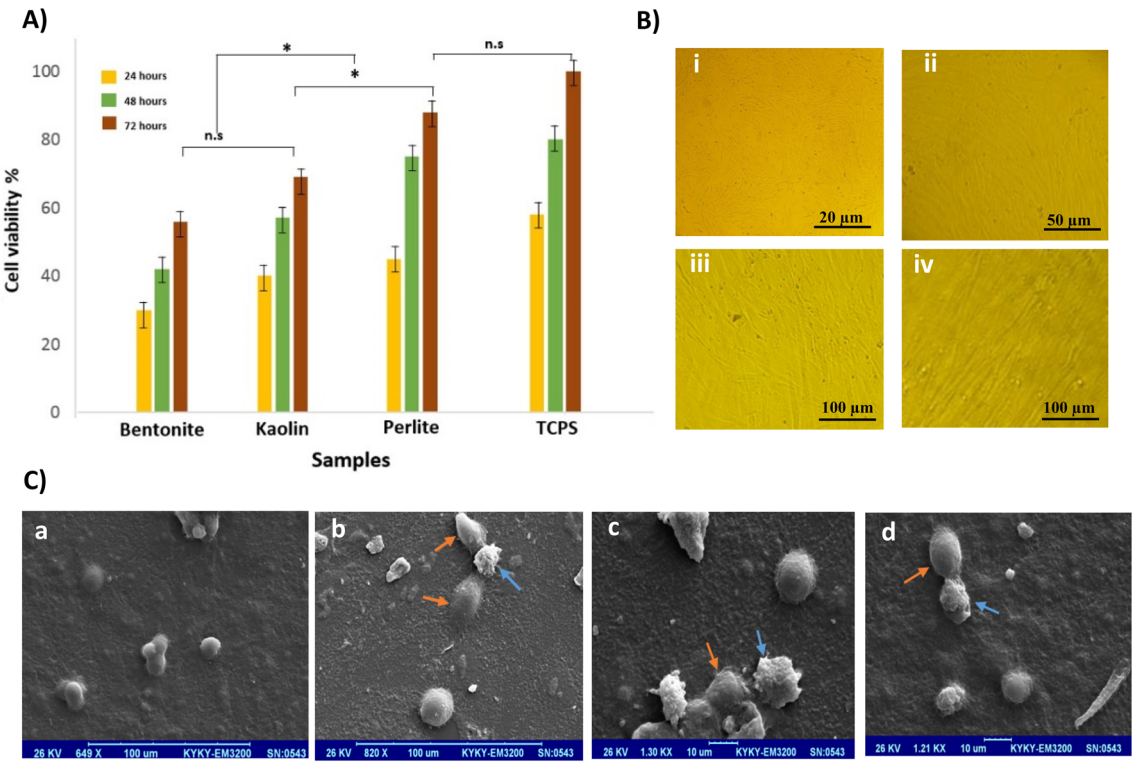

Fig. 3 Cell studies. (A) MTT results of samples with fibroblast cells at different times ($p < 0.01$). (B) Light microscopic images of fibroblast cells cultured on samples, (i) Control (TCPS), (ii) Perlite, (iii) Kaolin, and (iv) Bentonite. (C) SEM images from cells cultured on samples. (a) Control (TCPS), (b) Perlite, (c) Kaolin, and (d) Bentonite.

in a time group and $p < 0.01$ between groups were investigated using Student's *t*-test and two-way analysis of variance (ANOVA) with Tukey's *post hoc* multiple comparison test for all groups.

3. Results and discussion

Some of the combinations consisting of clays from XRF analysis showed in Table 1. The highest amounts of silicon dioxide and aluminum oxide as the two primary compounds of aluminosilicates were obtained in perlite and kaolin, respectively. The morphology of the clays was showed in Fig. 2. Clays show flat-layered structures which are made of particles in micrometer dimensions (5–10 μm).[46]

The specific surface area, pore volume, and pore size of clays were determined by BET analysis (Table 2). Perlite showed the highest specific surface area of 26 $m^2\ g^{-1}$, while for kaolin and bentonite, it was 17 and 14 $m^2\ g^{-1}$, respectively. The spacing of the layered structures was smaller in the case of bentonite and kaolin, which resulted in smaller differences between the specific surface areas. The pore volume was 2.07 $cm^3\ g^{-1}$, and the pore diameter was about 15 nm for perlite powder, while other clays had smaller & closer pores of approximately 3 nm.

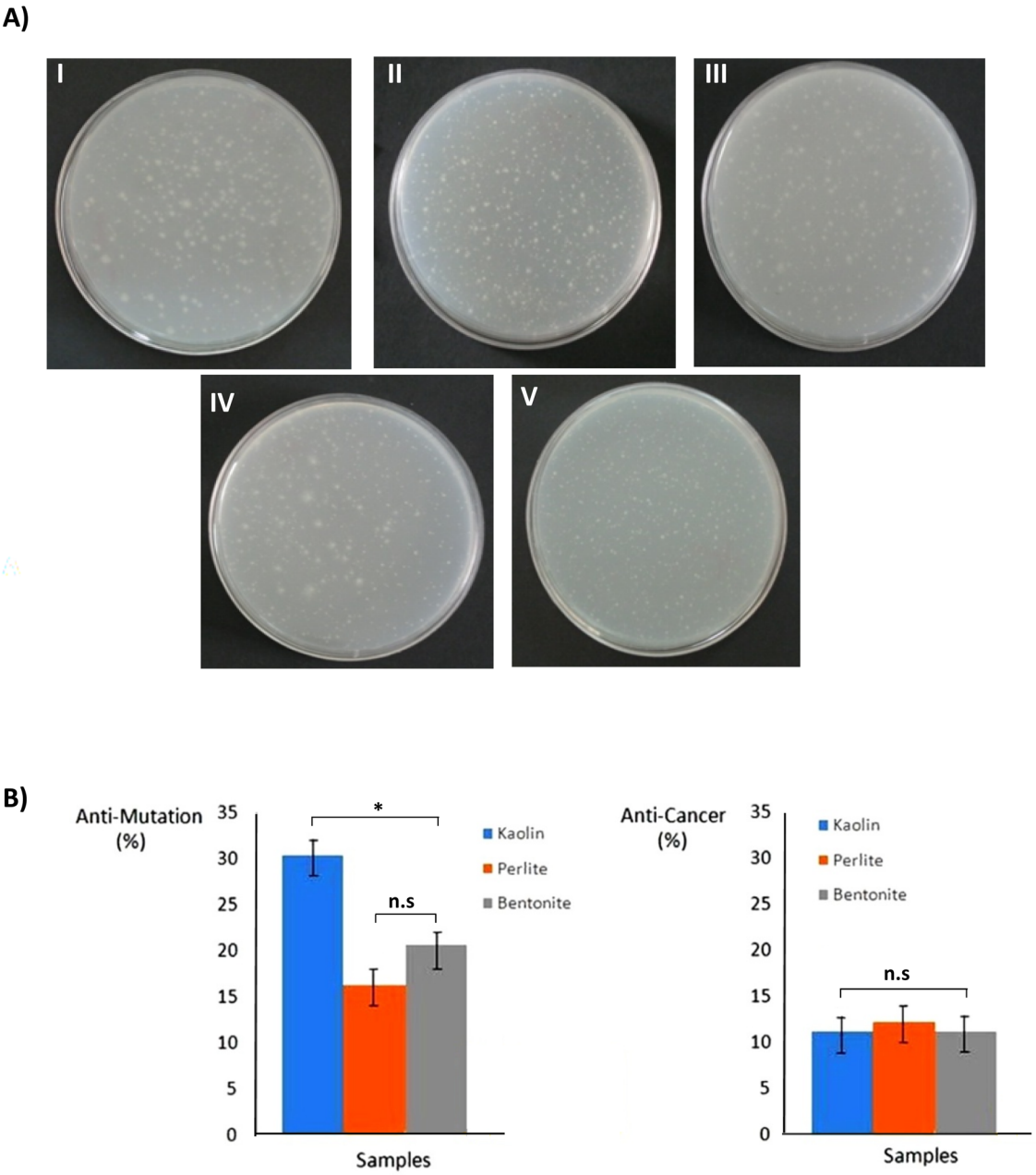

Fig. 4 Ames test of samples: the results of returned colonies (A) distilled water (negative control) (I), Perlite (II), Pentonite (III), Positive control (IV), and Paolin (V). (B) Anti-mutagenic and anti-cancer effect of powders against sodium azide (positive control) ($p < 0.01$). These results were obtained using one-way ANOVA method with $P < 0.01$.

Fig. 3A shows the MTT assay for TCPS (tissue culture polystyrene (control)), perlite, bentonite, and kaolin samples. Viability results of the powders showed that bentonite has the lowest viability, about 53%, kaolin at 70%, and perlite at 90%. Light microscopic images (Fig. 3B) illustrated the viability and proliferation of fibroblast cells on perlite and kaolin surfaces, and also SEM images indicated strong cell adherence, especially on perlite powders (Fig. 3C).

According to the Ames theory, if the number of colonies on the positive control medium (contained carcinogen) is two times more than in test samples, the substance will be considered anti-mutagenesis and anticancer. When prevention percent ranges between 25 and 40%, the mutagenesis effect in the test sample is assumed to be medium, and when it is more than 40%, the mutagenesis effect of the test sample is strong. If it is less than 25%, the mutagenesis effect is negative, which considers having an anticancer effect by adding S9 for metabolic activation.[44,45] Results showed that bentonite and perlite powders prevent the reverted mutations, and these mutagenesis effects were adverse, but kaolin powder mutagenesis effect was obtained medium (Fig. 4).

The potency of perlite, kaolin, and bentonite in promoting clot formation was evaluated by measuring the clotting time in plasma. The powders were dissolved in water and formed clear suspensions (Fig. 5A). The solubility results showed that perlite and bentonite have higher dispersion than kaolin powder. The

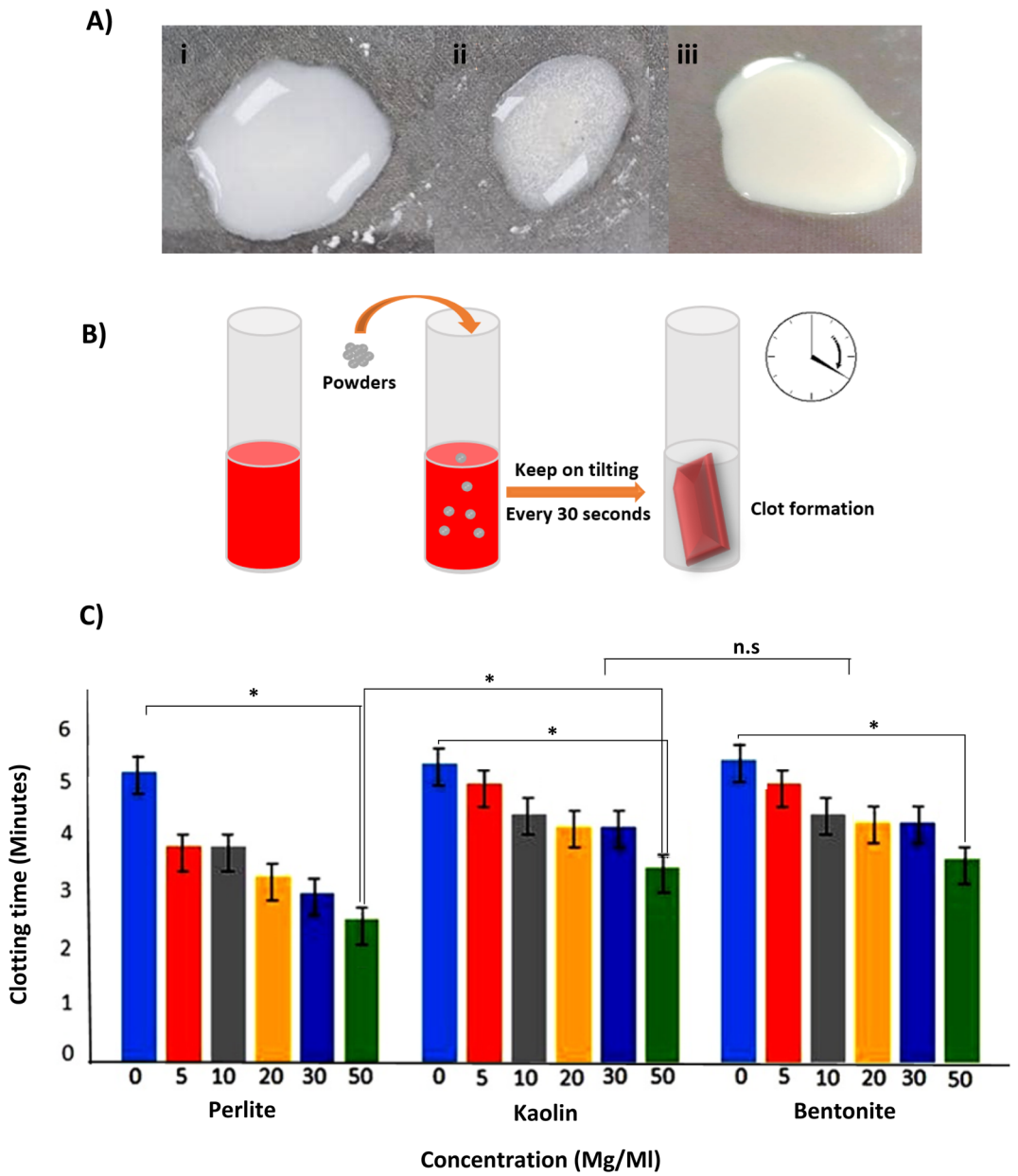

Fig. 5 (A) Solubility of powders in water, (i) Perlite, (ii) Kaolin, and (iii) Bentonite. (B) Schematic image of measurement method of clotting time. (C) Clotting times of powders in different concentrations ($p < 0.05$, $p < 0.01$).

solutions were transferred to tubes for coagulation assay (Fig. 5B). All the materials studied here reduced the clotting time compared to pure plasma (Fig. 5C). The CT results showed that the coagulation time for all samples decreased with the amount of powder. The lowest coagulation time of about 140 ± 2 seconds was obtained for pearlite with a powder concentration of 50 mg mL^{-1}, while this time was longer for other powders (control: 315 ± 2 seconds, kaolin: 192 ± 5 seconds, and bentonite: 202 ± 4 seconds for 50 mg mL^{-1}). Mortazavi *et al.*,[40] showed that the mean coagulation time in control blood samples was 253.4 seconds, whereas it was 149.5, 162.3and 143.4 seconds, respectively in blood samples treated with bentonite, zeolite, and CoolClot (bentonite–zeolite minerals).

Three types of powders, perlite, kaolin, and bentonite, can activate XII factor. The density and molecular weight of perlite were significantly lower than bentonite and kaolin, which is important in several aspects: its solubility was more than two other compounds, which had a better effect on the coagulation process. Changes in biochemical parameters such as glucose, urea, creatinine, alkaline phosphatase (Alk-P), magnesium, CPK, phosphorus, and LDH in blood and total protein were subtle and neglected data in the article. However, the powders could increase calcium, phosphorus, and LDH in the blood. Therefore, hemolysis results affect the results of SGOT, SGPT, and K and cause a false increase (Fig. 6).

The high surface reactivity of aluminosilicates and their wide range of possible interactions make this a sensational and fertile field of research for biomaterial design which, to date, remains relatively unexplored. Many studies have demonstrated the influence of aluminosilicates on mineralization processes which themselves exert upstream influences on cellular differentiation. The possible role of aluminosilicate amphoteric edge charges on cellular uptake and cell adhesion will be critically dependent on ambient ionic and pH conditions[46,47] and interactions with proteins, polymers, and other minerals may be tuned through modulation of aluminosilicate structure and cation exchange capacity.[48] As a result, the number of researches investigating the biocompatibility of aluminosilicates and their direct interactions with cells and tissues is growing. These studies have yielded random observations of aluminosilicate-dependent enhancements to cellular responses such as cell adhesion and differentiation. These materials have shown promise for bone tissue engineering applications.[49,50] The anisotropic and heterogeneous charge structures of aluminosilicate particles and their aggregates and the silica affinity for calcium ions[51] may provide favorable nucleation sites facilitating Ca^{2+} and HPO_4^{2-} adsorption to lessen the energy barrier for calcium phosphate deposition.[52] Ostomel *et al.* demonstrated that parameters such as the surface charge of the inorganic oxides like aluminosilicates could accelerate hemostatic *via* protein activation.[53] In addition, these minerals can separate water from the blood. In other words, water is trapped in pores of aluminosilicates because of its surface charge; additionally, the matrix within these compounds and

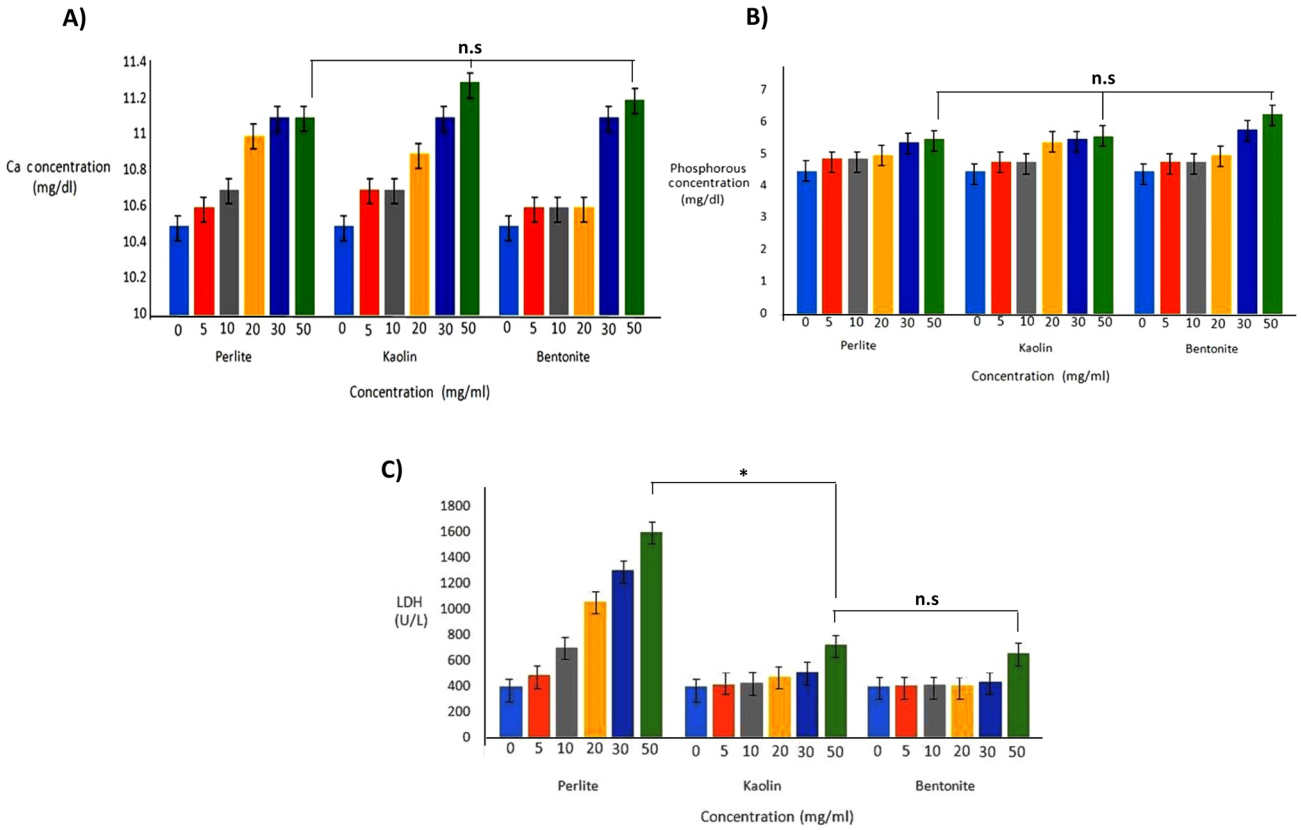

Fig. 6 Calcium (A) and phosphorous (B) and LDH (C) concentrations of blood in the presence of different hemostatic agents ($p < 0.01$).

hydrogen bonding is involved in water molecules' retention. This function increases the density of blood cells and giant proteins, so coagulation is catalyzed.[53] Generally, because of negative charges on the aluminosilicates' surfaces, they can absorb factor XII (Hageman factor) and activate it, so they significantly affect the extrinsic pathway of blood coagulation; thus, the coagulation time is reduced dramatically. So, these organic materials can be introduced as a quick coagulant in severe hemorrhages.[54] Perlite was in the ideal condition regarding its inhibitory effect on DNA mutations, which indicates a supportive property. In this regard, not only kaolin, bentonite and perlite had no mutagenic and carcinogenic effects, but also some anti-mutation and anti-tumor effects were shown. Due to their particular structure, chemical formula, and electrical charges, these materials can activate the intrinsic coagulation pathway by activating factor, XII. Thus, factor XII activates factor XI in the presence of prekallikrein (or Fletcher 6 factor) and HMWK (or Fitzgerald factor) and eventually leads to the formation of the fibrin matrix. Therefore, the XII factor can be activated by polyanionic surfaces like glasses and mineral constituents such as silica, perlite, kaolin, *etc.* The growth of blood's calcium and phosphorus is due to the presence of such ions in the perlite. The presence of calcium ions is very effective in the coagulation process, so these ions can be one of the main reasons for reducing the clotting time of perlite. One of the disadvantages of perlite is the increase in blood LDH levels, but with control methods such as using bandages and material coatings instead of powder, the release of powders into the blood can be prevented. These data suggest that the future clearance of mineral-based hemostatic agents should require more extensive cytotoxicity testing than the current Food and Drug Administration requirements.

4. Conclusion

In this study, the physical & biological properties and hemostatic effects of three types of aluminosilicate ceramics were investigated. For the first time, the results of this study demonstrated that perlite is beneficial as a biocompatible material and non-toxic with suitable morphological properties. The high specific surface area, suitable pores, high viability, good anti-cancerous nature can differentiate it than other studied materials. High specific surface area, suitable pores, high viability, anti-cancer nature of perlite can distinguish it from other studied materials. The CT results showed that materials such as kaolin, bentonite, and especially perlite reduce the clotting time up to 1.5–2 times and cause the activation of coagulation factors. Such inexpensive materials can be used in various shapes and applications, such as heavy bleeding bandages, dressings, and test tubes.

Conflicts of interest

The authors declare that they have no known competing financial interests or personal relationships that could have appeared to influence the work reported in this paper.

References

1 K. Robinson, Controlling Bleeding in the Field: Hemostatic Powders and Dressings Debut in the Prehospital Setting, *J. Emerg. Nurs.*, 2004, **30**, 160–161.
2 M. C. Neuffer, J. McDivitt, D. Rose, K. King, C. C. Cloonan and J. S. Vayer, Hemostatic Dressings for the First Responder: A Review, *Mil. Med.*, 2004, **169**, 716–720.
3 F. Vestergaard Rikke, H. Nielsen Per, A. Terp Kim, K. Søballe, G. Andersen and M. Hasenkam John, Effect of Hemostatic Material on Sternal Healing After Cardiac Surgery, *Ann. Thorac. Surg.*, 2014, **97**(1), 153–160.
4 H. Seyednejad, M. Imani, T. Jamieson and A. M. Seifalian, Topical Haemostatic Agents, *Br. J. Surg.*, 2008, **95**, 1197–1225.
5 R. Stewart, J. Myers, D. Dent, P. Ermis, G. A. Gray, R. Villarreal and et al, ., Seven Hundred Fifty-Three Consecutive Deaths in a Level I Trauma Center: The Argument for Injury Prevention, *J. Trauma*, 2003, **54**, 66–71.
6 H. Champion, R. Bellamy, C. Roberts and A. Leppaniemi, A Profile of Combat Injury, *J. Trauma*, 2003, **54**, 13–19.
7 J. Hurler and N. Skalko-Basnet, Potentials of Chitosan-Based Delivery Systems in Wound Therapy: Bioadhesion Study, *J. Funct. Biomater.*, 2012, **3**, 37–48.
8 Y. Zheng, J. Wu, Y. Zhu and C. Wu, Inorganic-based biomaterials for rapid hemostasis and wound healing, *Chem. Sci.*, 2023, **14**, 29–53.
9 Y. Ikeda, L. Young, J. Vournakis and A. Lefer, Vascular Effects of Poly-N-Acetylglucosamine in Isolated Rat Aortic Rings, *J. Surg. Res.*, 2002, **102**, 215–220.
10 M. Jackson, M. Taher, J. Burge, C. Krishnamurti, T. Reid and B. Alving, Hemostatic Efficacy of a Fibrin Sealant Dressing in an Animal Model of Kidney Injury, *J. Trauma*, 1998, **45**, 662–665.
11 R. Roth, Making Absorbable Surgical Felt, *US Pat.*4128612, 1978.
12 G. Ersoy, M. Kaynak, O. Firat Yilmaz, U. Rodoplu, F. Maltepe and N. Gokmen, Hemostatic effects of microporous polysaccharide hemosphere in a rat model with severe femoral artery bleeding, *Adv. Ther.*, 2007, **24**(3), 485–492.
13 L. Murat Francois-Joseph, Q. Le Carter, H. Ereth Mark, P. Piedra Mark, Y. Dong and T. Gettman Matthew, Evaluation of Microporous Polysaccharide Hemispheres as a Novel Hemostatic Agent in Open Partial Nephrectomy: Favorable Experimental Results in the Porcine Model, *J. Urol.*, 2004, **172**(3), 1119–1122.
14 D. Horák, F. Svec and J. Kalal, Hydrogels in Endovascular Embolization. I. Spherical Particles of Poly(2-Hydroxyethyl Methacrylate) and Their Medico-Biological Properties, *Biomaterials*, 1986, **7**, 188–192.
15 H. B. Alam, Z. Chen, A. Jaskille, R. I. Querol, E. Koustova, R. Inocencio and et al, ., Application of a Zeolite Hemostatic Agent Achieves 100% Survival in a Lethal Model of Complex Groin Injury in Swine, *J. Trauma*, 2004, **56**, 974–983.
16 D. Horak, M. Metalova and F. Svec, Hydrogels in Endovascular Embolization. Iii. Radiopaque Spherical

Particles, Their Preparation and Properties, *Biomaterials*, 1987, **8**, 142–145.

17 T. Sugamori, H. Iwase, M. Maeda, Y. Inoue and H. Kurosawa, Local Hemostatic Effects of Microcrystalline Partially Deacetylated Chitin Hydrochloride, *J. Biomed. Mater. Res.*, 2000, **49**, 225–232.

18 I. Masayuki, Photocrosslinkable Chitosan Hydrogel as a Wound Dressing and a Biological Adhesive, *Trends Glycosci. Glycotechnol.*, 2002, **14**, 331–341.

19 A. Hoekstra, H. Struszczyk and O. Kivekäs, Percutaneous Microcrystalline Chitosan Application for Sealing Arterial Puncture Sites, *Biomaterials*, 1998, **19**, 1467–1471.

20 D. Jensen, G. Machicado and K. Hirabayashi, Randomized Double-Blind Studies of Polysaccharide Gel Compared with Glue and Other Agents for Hemostasis of Large Veins and Bleeding Canine Esophageal or Gastric Varices, *J. Trauma*, 2004, **57**, 33–37.

21 D. Albala, Fibrin Sealants in Clinical Practice, *J. Cardiovasc. Surg.*, 2003, **11**, 5–11.

22 D. G. Wallace, G. M. Cruise and W. M. Rhee, A Tissue Sealant Based on Reactive Multifunctional Polyethylene Glycol, *J. Biomed. Mater. Res.*, 2001, **58**, 545–555.

23 S. Jiang, S. Liu, S. Lau and J. Li, Hemostatic biomaterials to halt non-compressible hemorrhage, *J. Mater. Chem. B*, 2022, **10**, 7239–7259.

24 G. Bao, Q. Gao, M. Cau, N. Ali-Mohamad and et al, ., Liquid-infused microstructured bioadhesives halt non-compressible hemorrhage, *Nat. Commun.*, 2022, **13**, 503re5, DOI: **10.1038/s41467-022-32803-1**.

25 T. V. Thamaraiselvi and S. Rajeswari, Biological Evaluation of Bioceramic Materials - a Review, *Trends Biomater. Artif. Organs*, 2004, **18**, 9–17.

26 D. D. Muehrcke, P. Barberi and W. M. Shimp, Calcium Phosphate Cements to Control Bleeding in Osteoporotic Sternums, *Ann. Thorac. Surg.*, 2007, **84**, 259–261.

27 Y. Momota, Y. Miyamoto, K. Ishikawa, M. Takechi and et al, ., Effects of Neutral Sodium Hydrogen Phosphate on the Setting Property and Hemostatic Ability of Hydroxyapatite Putty as a Local Hemostatic Agent for Bone, *J. Biomed. Mater. Res., Part B*, 2004, **69**, 99–103.

28 D. Georgiev, B. Bogdanov, I. Markovska and Y. Hristov, A study on the synthesis and structure of zeolite nax, *J. Chem. Technol. Metall.*, 2013, **48**(2), 168–173.

29 A. E. Pusateri, A. V. Delgado, E. J. Dick, R. S. Martinez, J. B. Holcomb and K. L. Ryan, Application of a granular mineral-based hemostatic agent (QuikClot) to reduce blood loss after grade V liver injury in swine, *J. Trauma*, 2004, **57**, 555–562.

30 F. L. Wright, H. T. Hua, G. Velmahos, D. Thoman, D. Demitriades and P. M. Rhee, Intracorporeal Use of the Hemostatic Agent Quickclot in a Coagulopathic Patient with Combined Thoracoabdominal Penetrating Trauma, *J. Trauma: Inj., Infect., Crit. Care*, 2004, **56**, 205–208.

31 J. K. Wright, J. Kalns, E. A. Wolf, F. Traweek, S. Schwarz, C. K. Loeffler and et al, ., Thermal Injury Resulting from Application of a Granular Mineral Hemostatic Agent, *J. Trauma: Inj., Infect., Crit. Care*, 2004, **57**, 224–230.

32 E. M. Acheson, B. S. Kheirabadi, R. Deguzman, E. J. Dick and J. B. Holcomb, Comparison hemorrhage control agents applied to lethal extremity arterial hemorrhages in swine, *J. Trauma*, 2005, **59**, 865–874.

33 P. Rhee, C. Brown, M. Martin, A. Salim, D. Plurad, D. Green and et al, ., QuikClot use in trauma for hemorrhage control: case series of 103 documented uses, *J. Trauma*, 2008, **64**, 1093–1099.

34 E. D. Cox, M. A. Schreiber, J. McManus, C. E. Wade and J. B. Holcomb, New hemostatic agents in the combat setting, *Transfusion*, 2009, **49**, 248S–255S.

35 P. Syrillos, J. H. Howe, D. A. C. Manning and S. D. Burley, Geological shape and controls on Kaolin particle consequences for mineral processing, *Clay Miner.*, 1999, **34**, 193–208.

36 B. S. Kheirabadi, R. Scherer Michael, J. Scot Estep, A. Dubick Michael and B. Holcomb John, Determination of Efficacy of New Hemostatic Dressings in a Model of Extremity Arterial Hemorrhage in Swine, *J. Trauma*, 2009, **67**, 450–460.

37 B. S. Kheirabadi, E. Mace James, B. Terrazas Irasema, G. Fedyk Chriselda, J. S. Estep, M. A. Dubick and et al, ., Safety Evaluation of New Hemostatic Agents, Smectite Granules, and Kaolin-Coated Gauze in a Vascular Injury Wound Model in Swine, *J. Trauma*, 2010, **68**, 269–278.

38 O. Demirbas, M. Alkan and M. Dogan, The removal of victoria blue from aqueous by adsorption on a low-cost material, *Adsorption*, 2002, **8**, 341–349.

39 A. C. Storm, T. Sawas, T. Higgins, D. H. Bruining, C. L. Leggett, N. S. Buttar and et al, ., Step-by-step use of hemostatic powder: treatment of a bleeding GI stromal tumor, *VideoGIE*, 2018, **23.4**(1), 5–6.

40 S. Mortazavi, A. Tavasoli, M. Atefi, N. Tanide, N. Radpey, P. Roshan-Shomal and et al, ., CoolClot, a novel hemostatic agent for controlling life-threatening arterial bleeding, *World J. Emerg. Med.*, 2013, **4**(2), 123–127.

41 B. S. Kheirabadi, M. R. Scherer, J. S. Estep, M. A. Dubick and J. B. Holcomb, Determination of efficacy of new hemostatic dressings in a model of extremity arterial hemorrhage in swine, *J. Trauma*, 2009, **67**, 450–460.

42 B. S. Kheirabadi, J. E. Mace, I. B. Terrazas, C. G. Fedyk, J. S. Estep, M. A. Dubick and L. H. Blackbourne, Safety evaluation of new hemostatic agents, smectite granules, and kaolin-coated gauze in a vascular injury wound model in swine, *J. Trauma*, 2010, **68**, 269–278.

43 P. D. Bowman, X. Wang, M. A. Meledeo, M. A. Dubick and B. S. Kheirabadi, Toxicity of aluminum silicates used in hemostatic dressings toward human umbilical veins endothelial cells, HeLa cells, and RAW267.4 mouse macrophages, *J. Trauma*, 2011, **71**(3), 727–732.

44 C. W. Chesterman, *Industrial Minerals and Rocks*, AIME, New York, 4th edn, 1975, p. 927.

45 D. R. Maron and B. N. Ames, Revised methods for the Salmonella mutagenicity test, *Mutat. Res.*, 1983, **113**, 173–215.

46 M. Delhorme, C. Labbez, C. Caillet and F. Thomas, Acid-base properties of 2:1 clays. I. modeling the role of electrostatics, *Langmuir*, 2010, **26**, 9240–9249.

47 C. Tournassat, J. Davis, A. Chiaberge, C. Grangeon and I. Bourg, Modeling the acid-base properties of montmorillonite edge surfaces, *Environ. Sci. Technol.*, 2016, **50**, 13436–13445.

48 W. H. Yu, N. Li, D. S. Tong, C. H. Zhou, C. X. Lin and C. Y. Xu, Adsorption of proteins and nucleic acids on clay minerals and their interactions: a review, *Appl. Clay Sci.*, 2013, **80–81**, 443–452.

49 A. H. Ambre, D. R. Katti and K. S. Katti, Biomineralized hydroxyapatite nanoclay composite scaffolds with polycaprolactone for stem cell-based bone tissue engineering, *J. Biomed. Mater. Res., Part A*, 2015, **103**, 2077–2101.

50 K. S. Katti, A. H. Ambre, S. Payne and D. R. Katti, Vesicular delivery of crystalline calcium minerals to ECM in biomineralized nanoclay composites, *Mater. Res. Express*, 2015, **2**, 45401.

51 M. S. Sadjadi, H. R. Ebrahimi, M. Meskinfam and K. Zare, Silica enhanced formation of hydroxyapatite nanocrystals in simulated body fluid (SBF) at 37 °C, *Mater. Chem. Phys.*, 2011, **130**, 67–71.

52 H. Henry Teng, How ions and molecules organize to form crystals, *Elements*, 2013, **9**, 189–194.

53 T. A. Ostomel, Oxide Hemostatic Activity, *J. Am. Chem. Soc.*, 2006, **128**, 8384–8385.

54 M. Naswir, S. Arita and M. Salni, Activation of Bentonite and application for reduction pH, color, organic substance, and Iron (Fe) in the peat water, *Sci. J. Chem.*, 2013, **1**(5), 74–82.